

Electrospinning of novel biodegradable poly(ester urethane)s and poly(ester urethane urea)s for soft tissue-engineering applications

Pablo C. Caracciolo · Vinoy Thomas · Yogesh K. Vohra ·
Fabián Buffa · Gustavo A. Abraham

Received: 5 March 2009 / Accepted: 24 April 2009 / Published online: 12 May 2009
© Springer Science+Business Media, LLC 2009

Abstract The development of biomimetic highly-porous scaffolds is essential for successful tissue engineering. Segmented poly(ester urethane)s and poly(ester urethane urea)s have been infrequently used for the fabrication of electrospun nanofibrous tissues, which is surprising because these polymers represent a very large variety of materials with tailored properties. This study reports the preparation of new electrospun elastomeric polyurethane scaffolds. Two novel segmented polyurethanes (SPU), synthesized from poly(ϵ -caprolactone) diol, 1,6-hexamethylene diisocyanate, and diester-diphenol or diurea-diol chain extenders, were used (Caracciolo et al. in *J Mater Sci Mater Med* 20:145–155, 2009). The spinnability and the morphology of the electrospun SPU scaffolds were investigated and discussed. The electrospinning parameters such as solution properties (polymer concentration and solvent) and processing parameters (applied electric field, needle to collector distance and solution flow rate) were optimized to achieve smooth, uniform bead-free fibers with diameter (~ 700 nm) mimicking the protein fibers of native extracellular matrix (ECM). The obtained elastomeric polyurethane scaffolds could be appropriate for soft tissue-engineering applications.

1 Introduction

The development of biomimetic highly-porous scaffolds is essential for successful tissue engineering. Nanofiber-based scaffolds prepared by electrospinning of biodegradable synthetic polymers not only mimic the nanoscale fibrous structure of natural extracellular matrix but also its spatial organization on the mesoscopic scale (control over fiber orientation and spatial placement).

Electrospinning or electrostatic spinning is a fiber spinning technique that recently emerged as a simple and promising technology for generating fibrous scaffolds for a wide range of biomedical applications such as drug delivery, wound dressing, vascular grafts, and tissue engineering matrices [1–4]. Specifically, electrospinning provides a mechanism to produce micro/nanofibrous scaffolds, non-woven nanostructured membranes, from a variety of polymeric materials, including both synthetic and natural polymers. The nanotopology of these electrospun scaffolds closely mimics that of native extracellular matrix (ECM). Fibers with diameters in the range from several micrometers down to less than 100 nm can be produced under a high-voltage electrostatic field operated between a metallic nozzle of a syringe and a metallic collector in air. The resulting nano/microfiber meshes have a very high surface area-to-volume ratio, and can be electrospun into three-dimensional scaffolds with very high porosity and interconnected pore structure. In this way, biomimetic matrices fabricated by electrospinning facilitate cell attachment, support cell growth, and regulate cell differentiation [5–8].

To date, electrospinning has been applied for the fabrication of nanofibrous scaffolds from numerous synthetic biodegradable polymers, such as poly(lactic acid) (PLA), poly(glycolic acid) (PGA), poly(ϵ -caprolactone) (PCL), polyhydroxybutyrate (PHB), as well as their blends,

P. C. Caracciolo · F. Buffa · G. A. Abraham (✉)
Instituto de Investigaciones en Ciencia y Tecnología de
Materiales, INTEMA (UNMDP-CONICET), Av. Juan B. Justo
4302, B7608FDQ Mar del Plata, Argentina
e-mail: gabraham@fi.mdp.edu.ar

V. Thomas (✉) · Y. K. Vohra
Department of Physics, Center for Nanoscale Materials and
Biointegration (CNMB), University of Alabama at Birmingham
(UAB), CH310, 1300 University Blvd, Birmingham,
AL 35294, USA
e-mail: vthomas@uab.edu

composites, and block copolymers [1]. These biodegradable polymers have been used to electrospin engineered scaffolds for bone tissue [9, 10], musculoskeletal tissue [11], myocardial tissue grafts [12, 13], and blood vessel substitutes [14, 15].

Segmented polyurethanes (SPU) and poly(urethane urea)s (SPUU) have been infrequently used for the fabrication of electrospun nanofibrous tissues, which is surprising because these polymers represent a very large variety of materials with tailored properties. So far, only limited studies on nanofibrous polyurethane scaffolds have been reported as tissue engineering scaffolds [16–19]. Biodegradation to non-toxic components may be promoted by the use of aliphatic diisocyanates in place of methylene bis-diphenylisocyanate (MDI). Moreover, there is an increasing need for elastomeric synthetic biodegradable materials that exhibit soft-tissue properties. For example, classical polyesters such as PGA, PLA, and their copolymers (PLGA) are relatively stiff, non-elastic materials and are not ideally suited for engineering of soft flexible tissues such as cardiovascular, urological, or gastrointestinal tissues. Scaffolds from elastomeric polyurethanes can withstand the action of stress and load and undergo an elastic recovery with little or no hysteresis. In recent years, a significant number of biocompatible and biodegradable SPU elastomers have been investigated [20, 21]. The highly variable chemistry of SPU allows the preparation of materials with controlled physico-chemical, mechanical, and biodegradation properties that can be achieved through the appropriate selection of monomers and hard and soft content manipulation.

Many applications of SPU in the tissue engineering field, such as cardiovascular tissue engineering [22–24], musculoskeletal applications (anterior cruciate ligament [25], knee joint meniscus [26], bone tissue engineering [27], smooth muscle cell constructs for contractile muscle [17, 28]), and nerve regeneration [29], have been recently evaluated. Although their potential for tissue regeneration and drug delivery has not been evaluated in vivo, biodegradable polyurethanes synthesized from aliphatic diisocyanates are emerging as scaffolds for regenerative medicine [21]. In a very recent in vivo rabbit study using a biodegradable polyesterurethane up to 63 days, Henry et al. [30] have shown that highly porous electrospun polyurethane scaffolds evoked a superior host tissue and angiogenic response compared to polyurethane membrane or film.

In previous papers Caracciolo et al. [31, 32] have reported the preparation, characterization, thermal and mechanical properties, and in vitro biological properties of aliphatic segmented polyurethanes based on PCL, hexamethylene diisocyanate (HDI), and novel aliphatic and aromatic chain extenders containing urea or ester functional groups, respectively. In the present work, a PCL-based

poly(ester urethane) and a PCL-based poly(ester urethane urea) were studied for electrospinnability into fibrous scaffolds under different solvents and spinning conditions. These two polymers were chosen because of their different composition and mechanical properties [32]. In order to optimize the conditions to create SPU nanofibers, parameters of the electrospinning process, such as solution properties (polymer concentration and solvent), and processing parameters (applied electric field, needle to collector distance and solution flow rate), were varied. The morphology of the obtained electrospun scaffolds based on novel SPU was investigated and discussed.

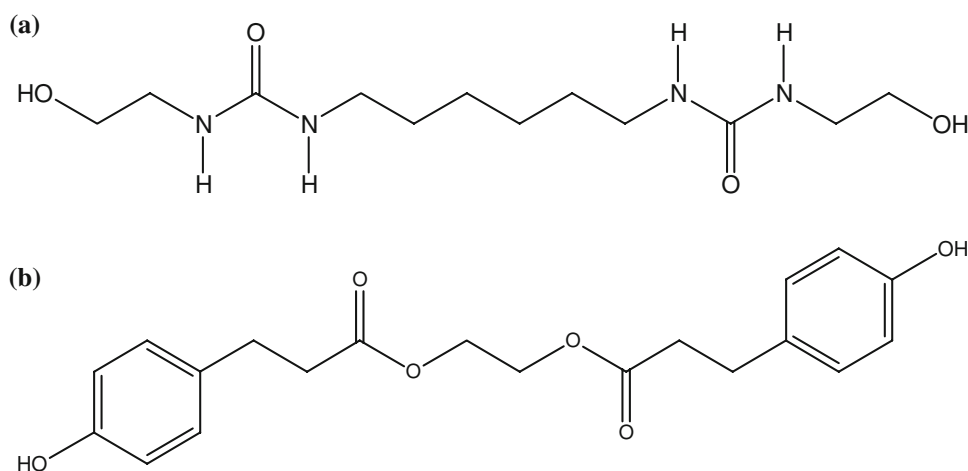
2 Materials and methods

2.1 Segmented polyurethanes synthesis

Macrodiol, chain extenders, and polyurethanes were synthesized according to previously reported procedures [32]. Briefly, PCL diol ($M_n = 2250$) was prepared by ring-opening polymerization of ϵ -caprolactone initiated by triethylene glycol. The aliphatic urea-diol chain extender (AE–H–AE) was synthesized from hexamethylene diisocyanate (HDI) and 2-aminoethanol at a molar ratio of 1:2. Scheme 1a shows the chemical structure of AE–H–AE. The reaction was carried out at 0°C with magnetic stirring and nitrogen flow. A tyrosine derivative was also prepared and used as diester-diphenol chain extender (D–E–D). This compound was synthesized by a Fischer esterification reaction between the carboxylic acid group of 3-(4-hydroxyphenyl)propionic acid (desaminotyrosine, DAT) and the hydroxyl groups of ethylene glycol catalyzed by *p*-toluene sulfonic acid in refluxing toluene. The reaction was driven towards completion by using a Dean-Stark apparatus to trap the evolved water. The chemical structure of D–E–D is shown in Scheme 1b.

SPU were obtained by a two-step polymerization method. Briefly, PCL diol was reacted with HDI in a 1:2.01 molar ratio at 80°C in anhydrous *N,N*-dimethylacetamide (DMAc) under stirring and nitrogen atmosphere. The pre-polymerization proceeded in the presence of dibutyltin dilaurate as catalyst (0.1 wt% of macrodiol) for 1 h, and then the solution was concentrated. The chain extenders were previously dissolved in DMAc, and added at a molar ratio 1:1 with respect to the prepolymer. Chain extension reaction proceeded for 6 h at 80°C. The resulting slurry was precipitated over cold distilled water, except for D–E–D-extended SPU which were precipitated over ether. Then, polymers were washed and dried under vacuum. The poly(ester urethane urea) and poly(ester urethane) samples were designated as PHH and PHD depending on the chain extender used (AE–H–AE or D–E–D, respectively).

Scheme 1 Chemical structures of synthesized chain extenders: **a** diurea-diol AE-H-AE, and **b** diester-diphenol D-E-D



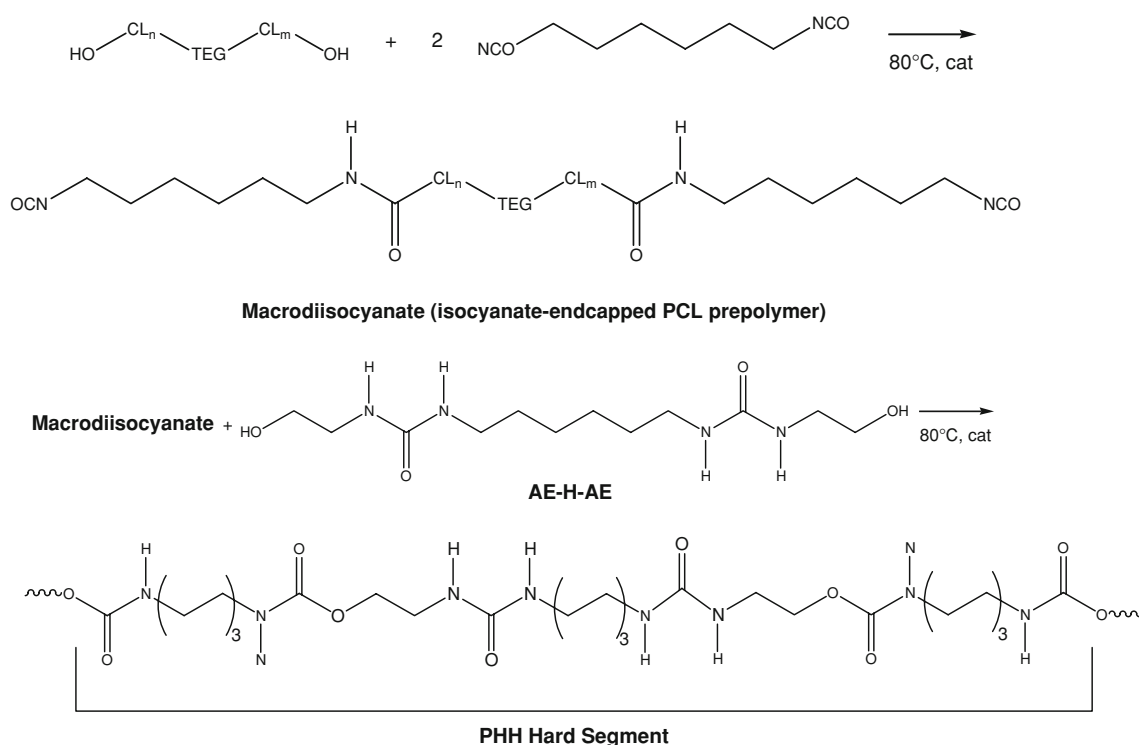
Scheme 2 displays the procedure followed in the case of PHH. Intrinsic viscosity $[\eta]$ measurements by means of an Ubbelohde Type OC viscosimeter (Cannon) using DMAc as solvent at $30 \pm 0.1^\circ\text{C}$ yielded the values of $[\eta]$ as 0.40 dl g^{-1} for PHH and 0.49 dl g^{-1} for PHD polymers.

2.2 Fibrous scaffold preparation and characterization

SPU solutions were prepared by dissolving SPU in different solvents and solvent mixtures on heating with stirring. DMAc, acetone (Ac), *N,N*-dimethylformamide (DMF), tetrahydrofuran (THF) and 1,1,1,3,3,3-hexafluoro-

2-propanol (HFP), were purchased from Aldrich Chemical Co., and used as solvents without further purification. The concentration of SPU solutions (C) was varied from 5 wt% to 30 wt% depending on the solvent used.

Each of the as-prepared solutions was loaded into a standard 10 ml plastic syringe connected to a polyamide tube, the open end of which was attached to a blunt 18-gauge stainless steel hypodermic needle (I.D. = 0.838 mm), which was used as the nozzle. A programmable syringe pump (Activa A22 ADOX S.A., Argentina) connected to the syringe controlled the flow rate. A high-voltage power source (ES30P, Gamma High Voltage Research Inc.) was



Scheme 2 Synthesis of poly(ester urethane urea) (PHH) by a two-step polymerization reaction

used to charge the solution by attaching the emitting electrode of positive polarity to the nozzle, and the grounding one to the aluminium collecting device. All experiments were carried out at room temperature in a chamber having a ventilation system.

The solutions were electrospun at a positive high-voltage (V) in a range of 10–20 kV, a working distance (h) of 10–20 cm (distance between the needle tip and the collecting plate), and a solution feeding rate (v) of 0.5–3 ml/h. The electrospun scaffolds were dried under vacuum at room temperature to fully eliminate the residual solvent, and stored in a desiccator.

The morphology of the electrospun SPU scaffolds was examined by scanning electron microscopy (SEM, JEOL Ltd., USA) at an accelerating voltage of 10 kV for fibrous specimens after gold sputtering. The average fiber diameter and diameter distribution were obtained by using an image-analyzer (Image-Pro Plus).

3 Results and discussion

Electrospinning is a unique and versatile process to produce polymeric fibers from polymer solutions and melts in the average diameter range of few nanometers to several micrometers (usually between 50 nm and 5 μm). The major attraction of this processing technique is its simplicity. However, electrospinning is governed by a number of parameters that greatly affect fiber formation and structure. Among these parameters are polymer molecular weight, polymer solution properties (concentration, solvent, viscosity, conductivity, and surface tension), applied electrical potential, polymer solution flow rate, distance between spinneret and collector (working distance), static or rotatory nature of the grounded target and ambient parameters (temperature, humidity, and air velocity). In order to produce defect-free nanofibers with controlled fiber diameter distribution and orientation, the above mentioned parameters have to be precisely controlled.

Far more than 100 different polymers of both natural and synthetic origin and their blends have been spun into nanofiber matrices [33]. Majority of these studies dealt with optimization of the electrospinning parameters to obtain nanofiber matrices with the desired properties [33].

In this work, the solution properties (concentration and solvent) and processing parameters (applied electric field, solution flow rate, and needle to collector distance) were examined. First, PHH solutions ($C = 5\text{--}40$ wt%) were prepared by using DMAc, and electrospun at $V = 10\text{--}20$ kV, $h = 10\text{--}20$ cm, and v of 0.5–3 ml/h. Figure 1 shows the morphology of electrospun PHH solutions. Only beads could be obtained for 30 wt% and lower concentrations. Figure 1a shows the nearly spherical microbeads with

diameters between 1.08 and 5.47 μm formed with $C = 30$ wt%. The beads are produced when the jet at the end of the Taylor cone splits into many mini-jets and each mini-jet disintegrates into small droplets, phenomena also referred to as electrospaying [34]. More concentrated solutions

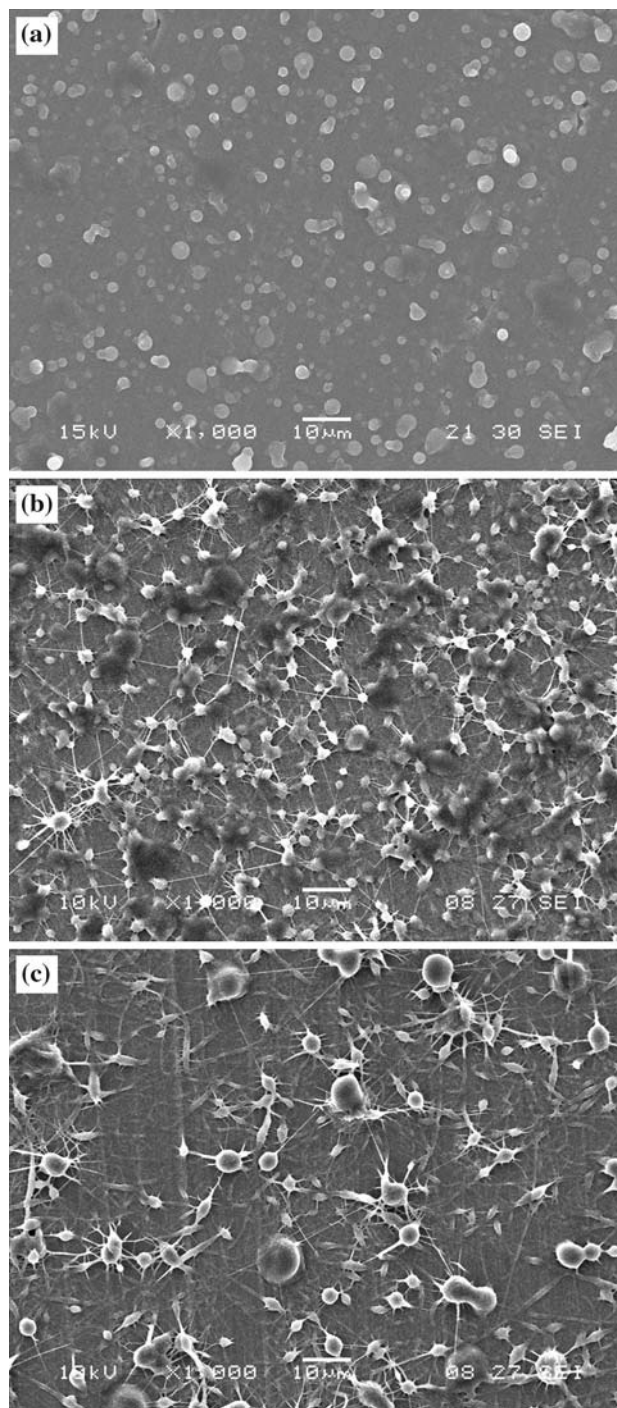


Fig. 1 SEM micrographs of electrospun PHH solutions at $v = 1$ ml/h, **a** $C = 30$ wt% in DMAc, $V = 12$ kV, $h = 15$ cm, **b** $C = 20$ wt% in DMAc/Ac (60/40), $V = 20$ kV, $h = 15$ cm, **c** $C = 20$ wt% in DMF/THF (50/50), $V = 20$ kV, $h = 15$ cm

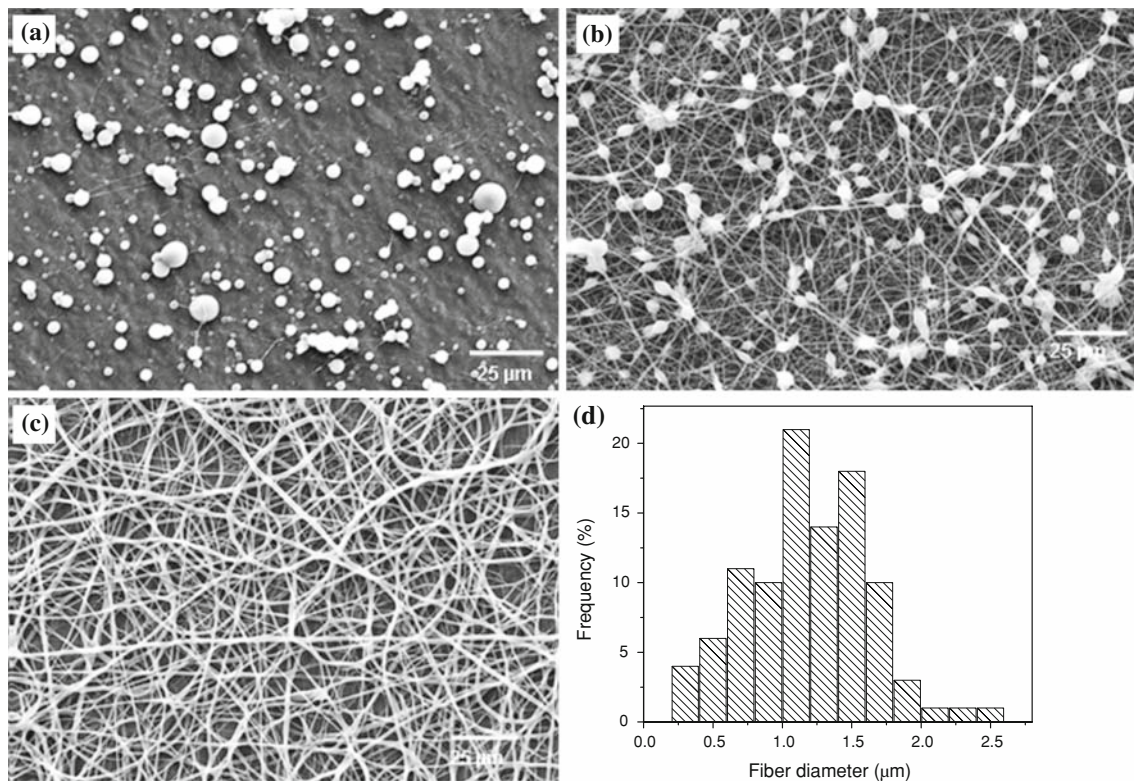


Fig. 2 SEM micrographs of electrospun PHH/HFP solutions, $v = 1$ ml/h, $V = 15$ kV, $h = 15$ cm at **a** $C = 10$ wt%; **b** $C = 15$ wt%; **c** $C = 20$ wt%; **d** Fiber diameter distribution corresponding to the scaffold showed in (c)

(40 wt% or higher) could not be processed by electrospinning due to the high viscosity achieved.

For highly hydrogen-bonded polymers such as polyurethanes, poly(urethane urea)s and polyamides, even in good solvents, the effect of polymer chain interactions on solution viscosity may not be neglected [35]. Thus, although DMAc is a good solvent for PHH, the presence of inter-chain hydrogen bonding is significant enough to affect solution viscosity, increasing the cohesiveness of the solution. The jet at the end of the Taylor cone did not undergo continuing and extensional flow, and then, electrospinning was prohibited.

When DMAc/Ac 60/40 solvent mixture was used, a morphology of beaded fibers was observed (Fig. 1b) for $C = 20$ wt%. Although acetone is not a good solvent itself for the samples, the DMAc/Ac mixture solubilizes the samples and introduces a lower boiling-point solvent which aided fiber formation. Solutions with concentrations higher than 20 wt% could not be electrospun into fibers due to the high viscosity achieved. In this case the solvent quality decreases, and the effects of polymer-polymer interactions on solution viscosity became increasingly important [35]. For the same SPU concentration the use of DMF/THF 50/50 as solvent mixture also allowed the formation of beaded fibers (Fig. 1c). An increase of solution concentration led to failure as the viscosity was too high.

When DMAc/Ac 60/40 solvent mixture was used, thinner fibers and smaller beads could be observed than in case of DMF/THF 50/50.

HFP has been reported to be a good solvent for electrospinning of highly hydrogen bonded proteins such as collagen [36, 37], gelatin [4, 38], and elastin [4, 38], hydrogen bonded polyamides [39], polyurethanes, and poly(urethane urea)s [40] though it is rather expensive. SPUU exhibit three-dimensional network of hydrogen bonding due to the inter-urea hydrogen bonding [41, 42] and are soluble only in highly polar organic solvents such as DMF, DMAc, and HFP. It shows that highly polar solvents are necessary for polyamides, proteins, and SPUU solubility and that hydrogen bonding between the hydrophilic part of proteins or polyurea hard segments in SPUU and common solvent molecules is not strong enough to break the inter-peptide or inter-urea hydrogen bonding interactions. Thus, HFP provided the highest electrospinnability of PHH, in which the hydroxyl group interacts with the hydrophilic hard segments of the SPUU by hydrogen bonding and the fluorine interacts with the hydrophobic soft segments of the SPUU. PHH/HFP solutions with concentrations ranging from 5 wt% to 20 wt% were used to spin PHH nanofibers. During the experimental process (1 kV/cm electric field strength and 1 ml/h solution flow rate), the jet broke into droplets; electrospaying instead of

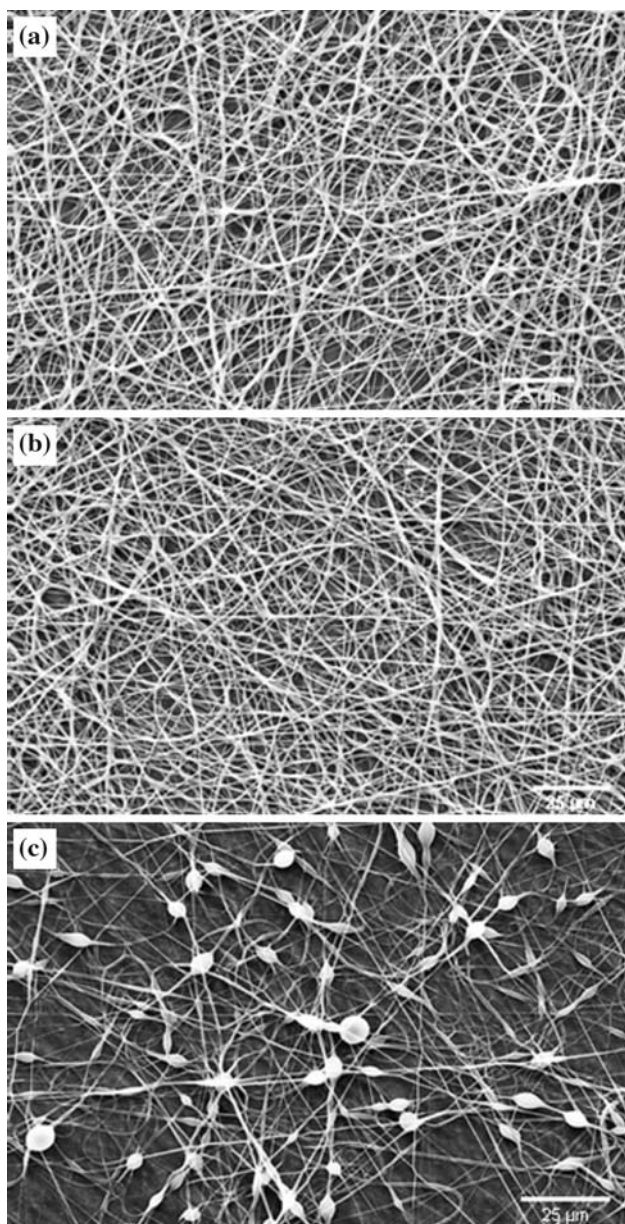


Fig. 3 SEM micrographs of electrospun PHH/HFP solutions, $C = 20$ wt%, $h = 15$ cm, at **a** $v = 2$ ml/h, $V = 15$ kV; **b** $v = 3$ ml/h, $V = 15$ kV; **c** $v = 1$ ml/h, $V = 10$ kV

electrospinning in the case of diluted solutions of PHH (≤ 10 wt%). This could be attributed to the lack of sufficient polymer-chain entanglements when the solution is too dilute (Fig. 2a). As the concentration increases to 15 wt%, the solution becomes viscoelastic and takes a longer time to break up into drops. As a result ‘bead-on-string’ morphology is formed (Fig. 2b). When the PHH/HFP concentration is above the critical concentration (C^*), polymer solution may form a network of entanglements, making the solution more elastic and electrospinnable into fibers. For PHH/HFP solution, the critical concentration is 20 wt% to form uniform fibers as seen in Fig. 2c. The resulting fiber

diameter average for the obtained scaffold was 1.22 ± 0.42 μm . The fiber diameter distribution is shown in Fig. 2d.

Figure 3a, b show the SEM images of the resultant nanofibers obtained by spinning 20 wt% PHH/HFP at higher feeding rates of the solution (2 and 3 ml/h). Usually a trend of increasing fiber diameter with increasing polymer solution feeding rate is expected in electrospinning. Contrary to this fact, SEM images of PHH scaffolds electrospun at a feeding rate of 1–3 ml/h showed an important decrease in the fiber diameter from 1.22 ± 0.42 μm for 1 ml/h to 0.75 ± 0.24 μm for 2 ml/h. This is because of the fact that the feeding rate affects the volume charge density and electrical current of a polymer solution as reported earlier [43]. The electrical current increases with the feeding rate increasing in certain polymer solutions, whereas it decreases with the feeding rate increasing in other polymer solutions. For example, it was observed by Theron et al. [44] that an increased feeding flow rate would increase the electrical current in poly(ethylene oxide), poly(vinyl acetate), poly(acrylic acid), and SPU solutions, whereas it reduced the electrical current in PCL solutions. Thus, increasing the feeding flow rate would decrease the fiber diameter, and thereby would decrease the surface charge density in the case of SPU polymers. However, a further increase in feeding rate to 3 ml/h did not show a significant change in fiber diameter (0.70 ± 0.20 μm). This result is also consistent with reports in the literature for other electrospun poly(ester urethane urea)s [40]. Figure 3c shows the SEM image of the nanofibers produced from the 20 wt% PHH/HFP solution at a lower applied voltage (10 kV), instead of 15 kV. It was found that uniform nanofibers without beads could not be obtained at the applied voltage of 10 kV in the case of PHH polymer.

PHD solutions were electrospun using the same range of concentrations and processing parameters explored in the case of PHH. Beaded morphologies from DMAc and DMAc/Ac solutions were formed independently of the concentration. However, in DMF/THF (50/50) solutions an effect of the concentration in the morphology was clearly observed. For $C = 10$ wt% only beads were formed (Fig. 4a). When the concentration was increased to $C = 20$ wt%, beads connected with nanofibers were obtained (Fig. 4b). Finally, an additional increase to $C = 30$ wt% allowed the formation of a bead-free fibrous structure (Fig. 4c) with a fiber diameter average of 1.31 ± 0.82 μm . The fiber diameter distribution (Fig. 4d) shows a bimodal distribution, indicating the presence of a mixture of two populations of fibers interpenetrated. The polymer concentration was high enough to cause chain entanglements with a low-enough viscosity to allow motion induced by the electric field. Higher solution concentrations led to failure as the viscosity was too high.

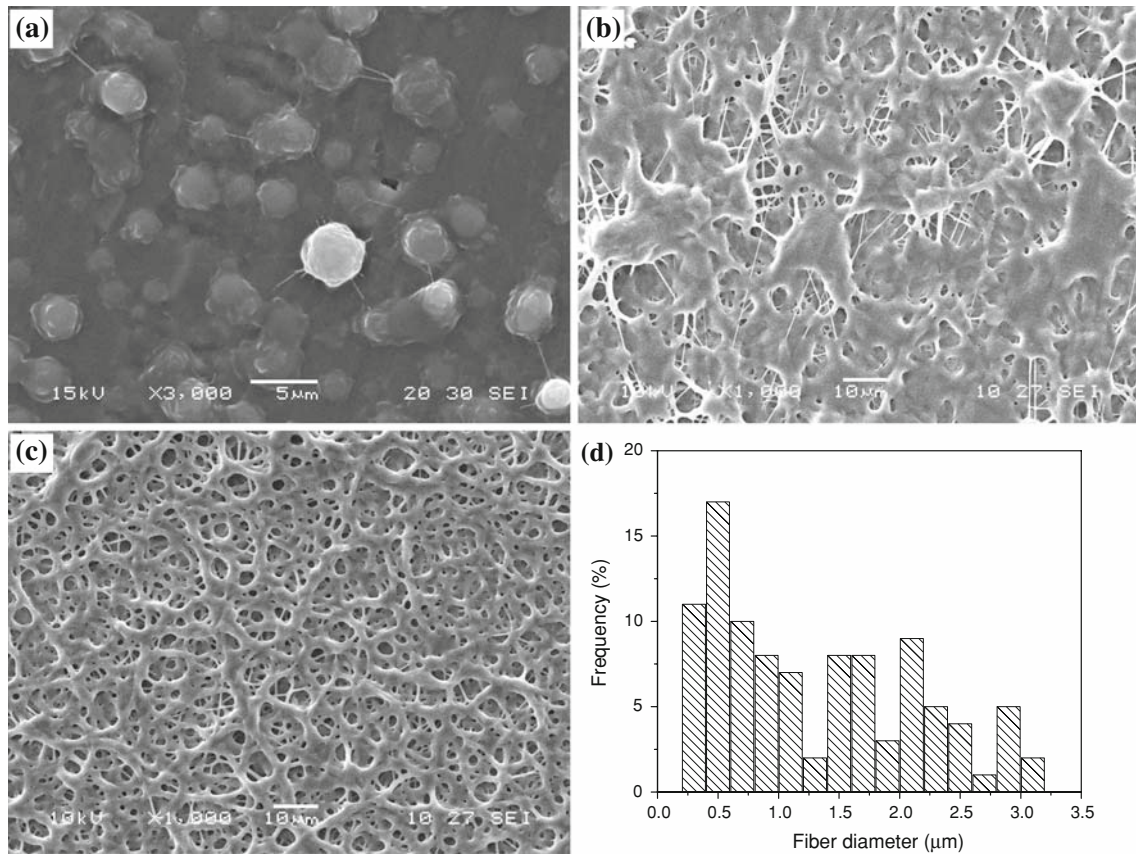
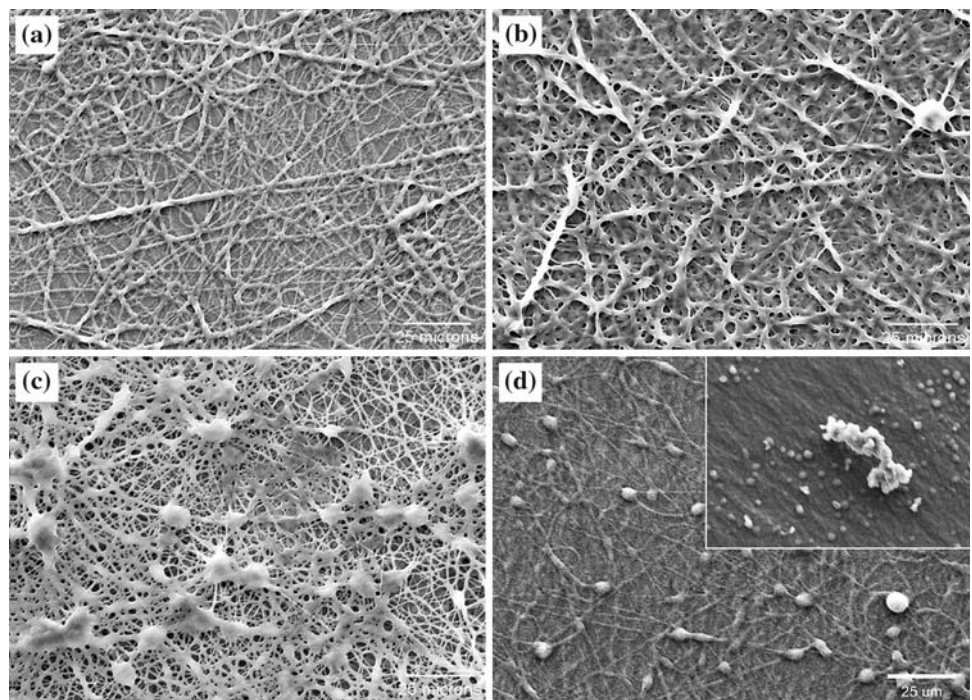


Fig. 4 SEM micrographs of electrospun PHD solutions in DMF/THF (50/50), $v = 1$ ml/h at **a** $C = 10$ wt%, $V = 20$ kV, $h = 15$ cm; **b** $C = 20$ wt%, $V = 15$ kV, $h = 10$ cm; **c** $C = 30$ wt%, $V = 20$ kV, $h = 15$ cm; **d** Fiber diameter distribution corresponding to the scaffold showed in (c)

Fig. 5 SEM micrographs of electrospun PHD/HFP solutions, $V = 15$ kV, $h = 15$ cm, at **a** $v = 0.5$ ml/h, $C = 20$ wt%; **b** $v = 1$ ml/h, $C = 20$ wt%; **c** $v = 2$ ml/h, $C = 20$ wt%; **d** $v = 1$ ml/h, $C = 15$ wt%. Inset in **d** shows bead formation at $v = 1$ ml/h, $C = 10$ wt%



PHD polymer was also electrospun using HFP as solvent. SEM images of electrospun PHD/HFP solutions are presented in Fig. 5. It was very difficult to spin a continuous fiber at a concentration below 20 wt% at 15 kV with a feeding rate of 0.5 ml/h and collector distance of 15 cm. Even though the solution could be successfully spun into polymer fibers at a concentration of 20 wt%, the resultant nanofibers were usually not uniform ($1.39 \pm 0.56 \mu\text{m}$) because of its high viscosity as seen in Fig. 5a. Moreover, due to the high viscous character of PHD polymer, the fibers formed during the spinning at a feeding rate of 1 ml/h were hard to dry before they reached the collecting screen (Fig. 5b). As a result, the fibers usually combined with one another through ‘point bonding’, showing an increase in fiber diameter average and distribution ($1.54 \pm 0.71 \mu\text{m}$). Electrospinning of 20 wt% PHD solution at a higher feeding rate (2 ml/h) has resulted in a mixture of beads (or drops) and nanofibers ($1.11 \pm 0.56 \mu\text{m}$) similar to those formed in the case of 15 wt% (Fig. 5c and d). The electrospinning of PHD/HFP solutions at $C \leq 10$ wt% under the same spinning conditions yielded only spherical beads ($4.49 \pm 0.71 \mu\text{m}$) as shown in the inset of Fig. 5d.

Based on the obtained results and focusing on the application of the synthesized SPU in the soft tissue-engineering field, mechanical characterization and in vitro degradation behavior is currently being investigated.

4 Conclusions

In this work, novel biodegradable segmented polyurethanes were successfully electrospun into engineered scaffolds appropriate for soft tissue-engineering applications. Solution properties (polymer concentration and solvent) and processing parameters (applied electric field, needle to collector distance and solution flow rate) were optimized to achieve smooth, uniform bead-free fibers. The influence of such processing parameters on the fiber morphology was investigated. It appears that HFP is a better solvent than DMF and THF for electrospinning the present polyurethanes.

Acknowledgments Y.K.V. and V.T. acknowledge the financial support from National Science Foundation, USA under the NSF-NIRT program with grant No. DMR-0402891. P.C.C. thanks to National Research Council (CONICET, Argentina) for the fellowship awarded. G.A.A. and F.B. acknowledge the financial support of National Agency for the Promotion of Science and Technology, CONICET, and National University of Mar del Plata (Argentina).

References

- Greiner A, Wendorff JH. *Angew Chem Int*. 2007;46:5670–703. doi:10.1002/anie.200604646.
- Lannutti J, Reneker D, Ma T, Tomasko D, Farson D. *Mater Sci Eng C*. 2007;27:504–9. doi:10.1016/j.msec.2006.05.019.
- Venugopal J, Zhang YZ, Ramakrishna S. *J Nanoeng Nanosyst*. 2004;218:35–45. doi:10.1243/174034905X39140.
- Thomas V, Zhang X, Catledge SA, Vohra YK. *Biomed Mater*. 2007;2:224–32. doi:10.1088/1748-6041/2/4/004.
- Pham QP, Sharma U, Mikos AG. *Tissue Eng*. 2006;12:1197–211. doi:10.1089/ten.2006.12.1197.
- Murugan R, Ramakrishna S. *Tissue Eng*. 2006;12:435–47. doi:10.1089/ten.2006.12.435.
- Liao S, Li B, Ma Z, Wei H, Chan C, Ramakrishna S. *Biomed Mater*. 2006;1:R45–53. doi:10.1088/1748-6041/1/3/R01.
- Thomas V, Dean DR, Vohra YK. *Curr Nanosci*. 2006;2:155–77.
- Yoshimoto H, Shin YM, Terai H, Vacanti JP. *Biomaterials*. 2003;24:2077–82. doi:10.1016/S0142-9612(02)00635-X.
- Shin M, Yoshimoto H, Vacanti JP. *Tissue Eng*. 2004;10:33–41. doi:10.1089/107632704322791673.
- Agrawal MC, Ray RB. *J Biomed Mater Res*. 2001;55:141–50. doi:10.1002/1097-4636(200105)55:2<141::AID-JBM1000>3.0.CO;2-J.
- Chen Q-Z, Bismarck A, Hansen U, Junaid S, Tran MQ, Harding SE, et al. *Biomaterials*. 2008;29:47–57. doi:10.1016/j.biomaterials.2007.09.010.
- Shin M, Ishii O, Sueda T, Vacanti JP. *Biomaterials*. 2004;25:3717–23. doi:10.1016/j.biomaterials.2003.10.055.
- Mo XM, Xu CY, Kotaki M, Ramakrishna S. *Biomaterials*. 2004;25:1883–90. doi:10.1016/j.biomaterials.2003.08.042.
- Xu CY, Inai R, Kotaki M, Ramakrishna S. *Biomaterials*. 2004;25:877–86. doi:10.1016/S0142-9612(03)00593-3.
- Riboldi SA, Sampaolesi M, Neuenschwander P, Cossu G, Mantero S. *Biomaterials*. 2005;26:4606–15. doi:10.1016/j.biomaterials.2004.11.035.
- Stankus JJ, Guan J, Fujimoto K, Wagner WR. *Biomaterials*. 2006;27:735–44. doi:10.1016/j.biomaterials.2005.06.020.
- Kidoaki S, Kwon IK, Matsuda T. *Biomaterials*. 2005;26:37–46. doi:10.1016/j.biomaterials.2004.01.063.
- Kidoaki S, Kwon IK, Matsuda T. *J Biomed Mater Res B Appl Biomater*. 2006;76B:219–29. doi:10.1002/jbm.b.30336.
- Gunatillake PA, Adhikari R. *Eur Cell Mater*. 2003;5:1–16.
- Guelcher SA. *Tissue Eng Part B*. 2008;14:3.
- Alperin C, Zandstra PW, Woodhouse KA. *Biomaterials*. 2005;26:7377–86. doi:10.1016/j.biomaterials.2005.05.064.
- Fujimoto KL, Guan J, Oshima H, Sakai T, Wagner WR. *Thorac Surg*. 2007;83:648–54. doi:10.1016/j.athoracsur.2006.06.085.
- Guan J, Fujimoto KL, Sacks MS, Wagner WR. *Biomaterials*. 2005;26:3961–71. doi:10.1016/j.biomaterials.2004.10.018.
- Gisselält K, Edberg B, Flodin P. *Biomacromolecules*. 2002;3:951–8. doi:10.1021/bm025535u.
- Heijkants RGJC, van Calck RV, van Tienen TG, de Groot JH, Buma P, Pennings AJ. *Biomaterials*. 2005;26:4219–28. doi:10.1016/j.biomaterials.2004.11.005.
- Kavlock KD, Pechar TW, Hollinger JO, Guelcher SA, Goldstein AS. *Acta Biomater*. 2007;3:475–84. doi:10.1016/j.actbio.2007.02.001.
- Riboldi SA, Sadr N, Pigiñi L, Neuenschwander P, Simonet M, Mogno P, et al. *J Biomed Mater Res*. 2008;84A:1094–101. doi:10.1002/jbm.a.31534.
- Borkenhagen M, Stoll RC, Neuenschwander P, Suter UW, Aebischer P. *Biomaterials*. 1998;19:2155–65. doi:10.1016/S0142-9612(98)00122-7.
- Henry JA, Burugapalli K, Neuenschwander P, Pandit A. *Acta Biomater*. 2009;5:29–42. doi:10.1016/j.actbio.2008.08.020.
- Caracciolo PC, de Queiroz AAA, Higa OZ, Buffa F, Abraham GA. *Acta Biomater*. 2008;4:976–88. doi:10.1016/j.actbio.2008.02.016.

32. Caracciolo PC, Buffa F, Abraham GA. *J Mater Sci Mater Med*. 2009;20:145–55. doi:[10.1007/s10856-008-3561-8](https://doi.org/10.1007/s10856-008-3561-8).
33. Huang Z-M, Zhang Y-Z, Kotaki M, Ramakrishna S. *Comp Sci Technol*. 2003;63:2223–53. doi:[10.1016/S0266-3538\(03\)00178-7](https://doi.org/10.1016/S0266-3538(03)00178-7).
34. Gupta P, Elkins C, Long TE, Wilkes GL. *Polymer (Guildf)*. 2005;46:4799–810.
35. Shenoy SL, Douglas Bates W, Frisch HL, Wnek GE. *Polymer (Guildf)*. 2005;46:3372–84. doi:[10.1016/j.polymer.2005.03.011](https://doi.org/10.1016/j.polymer.2005.03.011).
36. Matthews JA, Wnek GE, Simpson DG, Bowlin GL. *Biomacromolecules*. 2002;3:232–8. doi:[10.1021/bm015533u](https://doi.org/10.1021/bm015533u).
37. Thomas V, Dean DR, Jose MV, Mathew B, Chowdhury S, Vohra YK. *Biomacromolecules*. 2007;8:631–7. doi:[10.1021/bm060879w](https://doi.org/10.1021/bm060879w).
38. Li M, Mondrinos MJ, Gandhi MR, Ko FK, Weiss AS, Lelkes PI. *Biomaterials*. 2005;26:5999–6008. doi:[10.1016/j.biomaterials.2005.03.030](https://doi.org/10.1016/j.biomaterials.2005.03.030).
39. Jose MV, Steinert BW, Thomas V, Dean DR, Abdalla MA, Price G, et al. *Polymer (Guildf)*. 2007;48:1096–104. doi:[10.1016/j.polymer.2006.12.023](https://doi.org/10.1016/j.polymer.2006.12.023).
40. Stankus JJ, Guan J, Wagner WR. *J Biomed Mater Res*. 2004;70A:603–14. doi:[10.1002/jbm.a.30122](https://doi.org/10.1002/jbm.a.30122).
41. Thomas V, Jayabalan M. *J Biomed Mater Res*. 2001;56A:144–57. doi:[10.1002/1097-4636\(200107\)56:1<144::AID-JBM1079>3.0.CO;2-D](https://doi.org/10.1002/1097-4636(200107)56:1<144::AID-JBM1079>3.0.CO;2-D).
42. Thomas V, Jayabalan M. *Biomaterials*. 2002;23:273–82. doi:[10.1016/S0142-9612\(01\)00106-5](https://doi.org/10.1016/S0142-9612(01)00106-5).
43. Nasir M, Matsumoto H, Danno T, Minagawa M, Irisawa T, Shioya M, et al. *J Polym Sci Part B Polym Phys*. 2006;44:779–86. doi:[10.1002/polb.20737](https://doi.org/10.1002/polb.20737).
44. Theron SA, Zussman E, Yarin AL. *Polymer (Guildf)*. 2004;45:2017–30. doi:[10.1016/j.polymer.2004.01.024](https://doi.org/10.1016/j.polymer.2004.01.024).